ISSN 1392-1207. MECHANIKA. Vol. 30, No. 2, 2024: 177–182

Investigating the Impact of Flow Profile on Heat Transfer in Nanofluid Flow: A Numerical Study

Bilal LITOUCHE*, Billel REBAI, Khelifa MANSOURI*****
**University center Abdelhafid Boussouf, Mechanic and ElectroMechanic department, 43000, Mila, Algeria, E-mail: b.litouche@centre-univ-mila.dz*
***Abbes LAGHROUR University, Khenchela, 40000, Algeria, E-mail: billel.rebai@univ-khenchela.dz*
****Abbes LAGHROUR University, Khenchela, 40000, Algeria, E-mal: lmansouri.khelifa@univ-khenchela.dz*
https://doi.org/10.5755/j02.mech.34638

1. Introduction

Efficient thermal energy systems, including water heating, solar air conditioning, agro-alimentary product drying, and refrigeration machines, require materials that optimize their performance. Heat exchangers, crucial components in these systems, benefit from enhanced coefficients of convective transfer and reduced load loss. Introducing solid particles with high thermophysical properties, such as aluminum oxide (Al_2O_3), into the base fluid has been a promising approach to achieve high heat transfer efficiency. Nanofluids, characterized by superior thermal conductivity and heat transfer properties compared to conventional fluids, have garnered significant interest in scientific research [1-3]. However, the concentration of nanoparticles in the base fluid can lead to increased pressure drop due to elevated viscosity, necessitating careful consideration of this parameter. Extensive research has shown that higher temperatures and concentrations result in improved thermal conductivity and heat transfer [4-6]. Nonetheless, nanoparticle agglomeration remains a challenge in nanofluid technology, prompting the utilization of three methods to maintain stable suspensions and prevent sedimentation: chemical methods involving surfactants, physical methods utilizing ultrasonic waves, and electrical methods controlling pH levels [7, 8].

Nanofluids consist of base liquids, such as water, fat, ethylene glycol (EG), and engine oil, infused with nanoparticles ranging from 1 to 100 nm. Various nanoparticles, including multi-walled carbon nanotubes (MWCNTs), single-walled carbon nanotubes (SWCNTs), CuO, Cu, Al, Si, among others, possess distinct thermal conductivity properties, contributing to enhanced heat transfer efficiency [9-11]. The optimization of nanofluid performance relies on several key parameters, including volume fraction, thermal conductivity of nanoparticles and base fluid, nanoparticle size and shape, acidity, temperature, aspect ratio, additives, and clustering effects. Notably, cylindrical-shaped nanoparticles, particularly carbon nanotubes (CNTs), exhibit superior thermal conductivity compared to spherical-shaped nanofluids [12-21].

This numerical investigation aims to analyze the turbulent flow and heat transfer characteristics of Al_2O_3 nanofluid in a mini-channel featuring a sinusoidal ribbed wall. The study examines the influence of nanoparticle concentration and Reynolds number (ranging from 5000 to 20,000) on critical factors such as the mean Nusselt number, coefficient of friction, and performance index for both water and nanofluid. Through this analysis, insights into the behavior of nanofluids in such configurations can be gained, contributing to the optimization of heat transfer in thermal energy systems.

2. Geometry and thermophysical properties of nanofluids

The geometry represented in Fig. 1 is the field of study of this numerical research, it considered as horizontal tube with inner hydraulic diameter D_h = 10 mm and a total length L_T = 340 mm. In the purpose of enhancing the heat transfer and flow behavior of water/Al_2O_3 nanofluid in the studied geometrics, the sinusoidal shapes of rib of the inner surface of the wall had been used. The uniform heat flux (Q'') equal to 10^4 W/m^2 parallel to the Y axis is imposed on the channel wall of the test section which has a length L_2 = 108 mm. The channel inlet length L_1 = 200 mm, and the exit section has the length of L_3 = 32 mm. The space ratio (e/b) equal to 0, 0.25, 0.5 equal to 0, 0.25, 0.5 and 1 mm are studied. The inlet temperature of working fluid is T_{in} = 300 K, and inlet velocity changes based on varying Reynolds number ranging from 5 000 to 20 000, with a volume fraction of aluminum nanoparticle ranging from 0 to 6%. The sinusoidal function used for drawing the corrugate shape of the wall of the ribs is written as following:

$$y = a \ \sin\left(2\pi\left(x/b\right)\right), \tag{1}$$

where a = 1 mm and b = 6 mm.

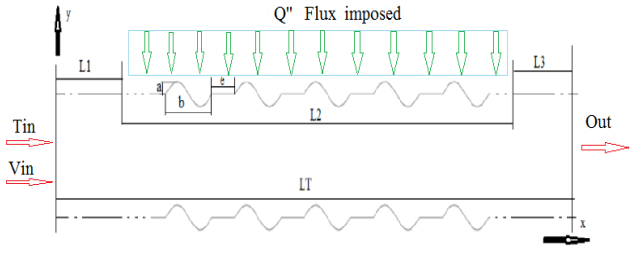

Fig. 1 Studied configuration

We take note that:

- If the ratio (e/b = 1) it means that $e = b$.
- If the ratio (e/b = 0.5) it means that $e = b/2$.

A simply to calculate the thermophysical properties of nanofluid such as density, specific heat, dynamic viscosity and thermal conductivity by considering the effects of nanoparticles and base fluid, the following equations are used [22].

Density:

$$\rho_{nf} = (1-\phi)\rho_f + \phi\rho_{np}. \quad (2)$$

Specific heat:

$$(\rho C_P)_{nf} = (1-\phi)(\rho C_P)_f + \phi(\rho C_P)_{np}, \quad (3)$$

where $(\rho C_P)_f$ and $(\rho C_P)_{np}$ are heat capacities of the based fluid and the solid nanoparticles, respectively.

Dynamic viscosity:

$$\mu_{nf} = \mu_f\left(123\phi^2 + 7.3\phi + 1\right). \quad (4)$$

Thermal conductivity:

$$k_{nf} = k_f\left(4.97\phi^2 + 2.72\phi + 1\right). \quad (5)$$

Table 1 below present properties of the nanofluid used in this study.

Table 1

The properties of nanofluids [23]

	φ	ρ	μ	Cp	k
Type of fluid	%	kg/m^3	MPa.s	J/kg.K	W/m.K
Pure water	0	997.7	0.949	4178.90	0.600
Al_2O_3/water	1	1027.4	1.020	4046.96	0.617
	2	1057.2	1.130	3922.46	0.635
	4	1116.6	1.410	3695.36	0.671
	6	1176	1.780	3487.42	0.709

3. Code validation

The numerical results have been validated with correlations of Dittus-Boelter and Blasius, respectively in terms of average Nusselt number and friction coefficients. The results are plotted in Fig. 2, a and Fig. 2, b.

Dittus-Boelter correlation [24]:

$$Nu_S = 0.023\,Re^{0.8}\,Pr^{0.4}. \quad (6)$$

Correlations of Blasius:

$$f = 0.316\,Re^{-0.25} \text{ for } (3*10^3 < Re < 2*10^4). \quad (7)$$

The comparison between the results of this study and previous works shows that the present numerical simulation is accurate because the results are in good agreement with the previous studies.

4. Results and discussion

The results reported in terms of average Nusselt number, friction coefficient, performance evaluation criteria index, as a function of Reynolds number ranging from 5000 to 20 000, roughness pitch values from *e/b* = 0 to 1, and particle volume concentrations of 1%, 2%, 4% and 6%.

4.1. Results of water working fluid

The variation of the Nusselt number profiles as a function of Reynolds number and space ratio *e/b* is presented in Fig. 3, the water is used as working fluid. It can be

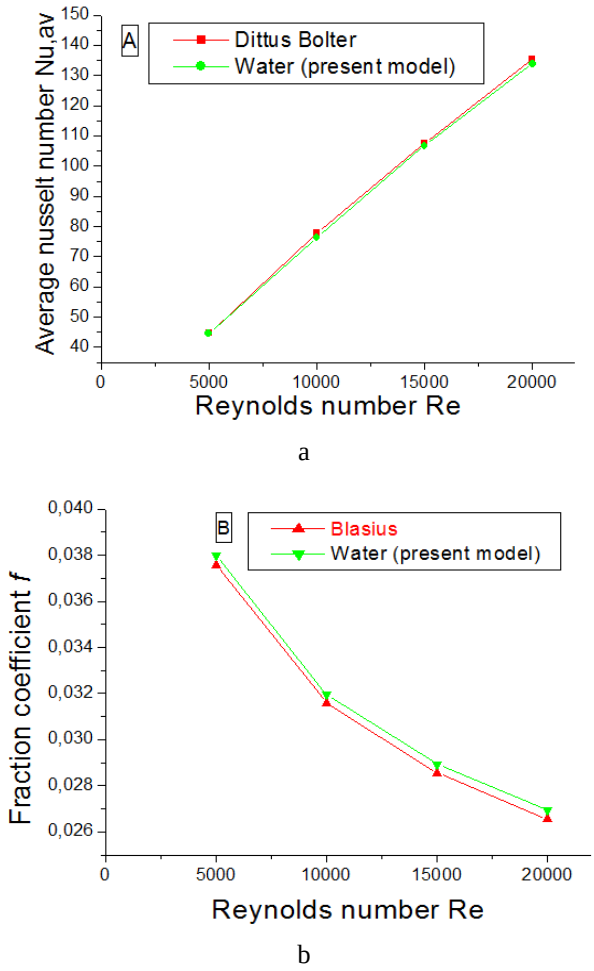

Fig. 2 Comparison of present results with equations of: a – Dittus-Boelter and b – Blasius; working fluid is water

seen that the Nusselt number increases with the increase in Reynolds number for all values of space ratio e/b in comparison with the smooth channel.

In Fig. 3, at the results show that the Nusselt number increases with 48,65% in case the space ratio *e/b* = 0 and 31,21%, 24,86%, 18,68%, in cases *e/b* = 0.25, *e/b* = 0.5, *e/b*=1 respectively. Thus, in Fig. 3, b we notice that there is an inverse relationship between friction coefficient and Reynolds number, the increase of the latter leads to the reduction in the coefficient of friction, the maximum values of the friction coefficient are noted for the space ratio case *e/b* = 0, where *f* = 0,041 for Reynolds number *Re* = 5000.

4.2. Results of Al_2O_3-water mixture (nanofluid) working fluid

- Case smooth channel

Fig. 4 shows the evaluation of the average Nusselt number in smooth channel with different volume fraction of nanoparticles and Reynolds number influenced by the presence of Aluminum particles in the water with different concentrations. It is clearly shown that the heat transfer mechanism improves by increasing volume fraction of nanoparticles. In Fig. 4, the average Nusselt number increases as Reynolds number increases, also that this quantity influenced by the presence of Aluminum particles in the water with different concentrations. It is clearly shown that the heat transfer mechanism improves by increasing volume fraction of

nanoparticles. Fig. 4, b shows the variation of friction factor with Reynolds number for different volume fraction of nanoparticles. It is seen that the particle volume concentrations of $\varphi = 0.06$ has the highest effect on friction factor and it is followed by $\varphi = 0.04$, 0.02 and 0.01respectively, and it is high at lower Reynolds number *Re* =5000. The results of this investigation study also shows that the average Nusselt number increases with 21.54% in case $\varphi = 0.06$ in comparison with $\varphi = 0.04$, 0.02 and 0.01where the height of values of Nusselt number is 21.54%, 16.16%, 10.18% and 8.86% respectively.

- Case channel with ribs

The combined effect of space ratio of ribs, φvales on the average Nusselt number, and fraction factor are presented in Fig. 5 and Fig. 6.

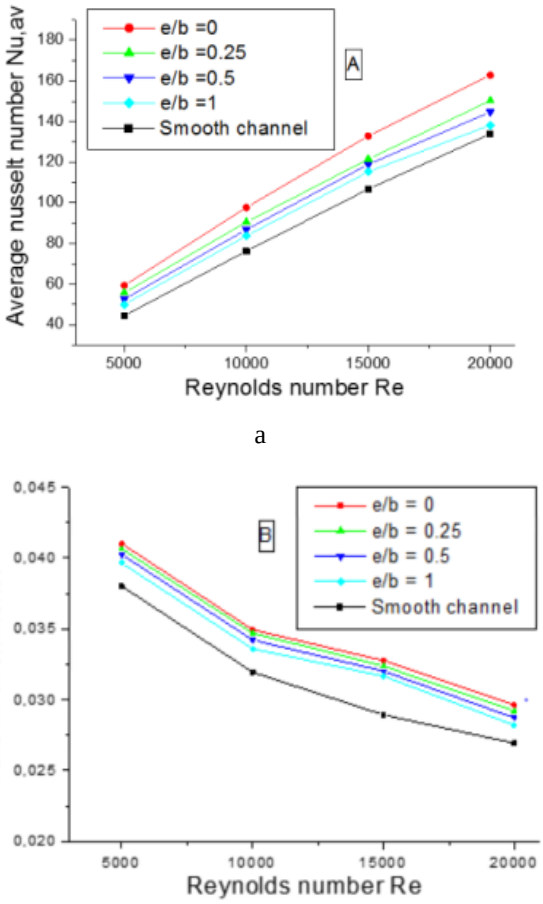

Fig. 3 Effect of space ratio on average Nusselt number (a) and friction factor (b); water is a working fluid

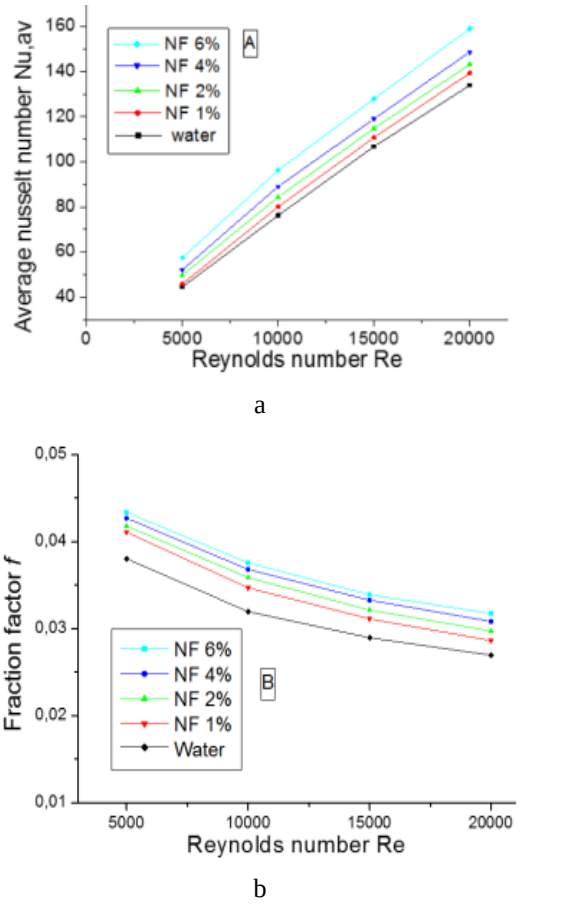

Fig. 4 Effect of different volume fraction nanoparticles with different Reynolds numbers on average: a – Nusselt number, b – friction factor (case smooth channel, Al_2O_3-water mixture)

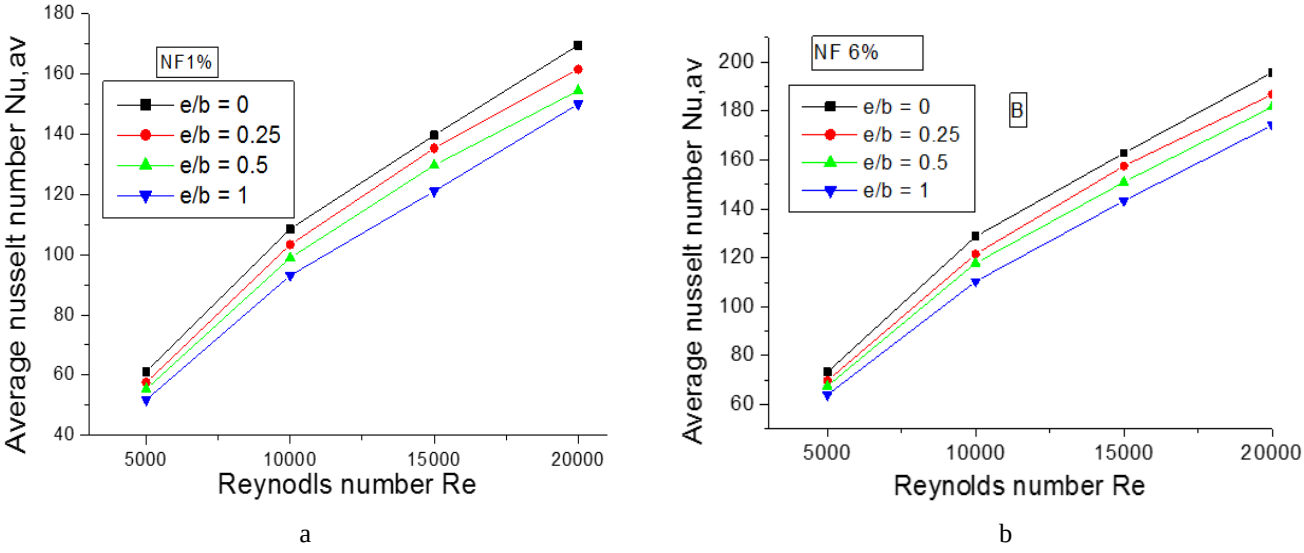

Fig. 5 Effectof space ratio with different Reynolds numbers on average Nusselt number: a – NF 1%, b – NF 6%

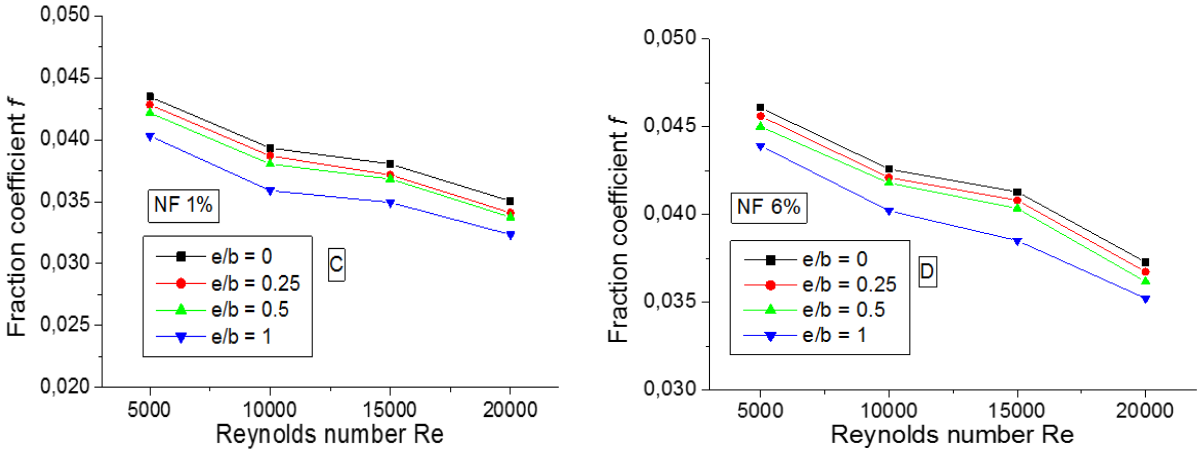

a b

Fig. 6 Effect of space ratio with different Reynolds numbers on fraction factor: a – NF 1%, b – NF 6%

It is observed that the distance between the undulations of ribs of the wall contributed to the reduction of the coefficient of friction. However, the average Nusselt numbers result enhanced by the employment of ribs surfaces and nanofluids. Also, it is observed that the space ratio *e/b* = 0 has the best heat transfer compared with other space ratios *e/b* = 0.25, 0.5 and 1 respectively.

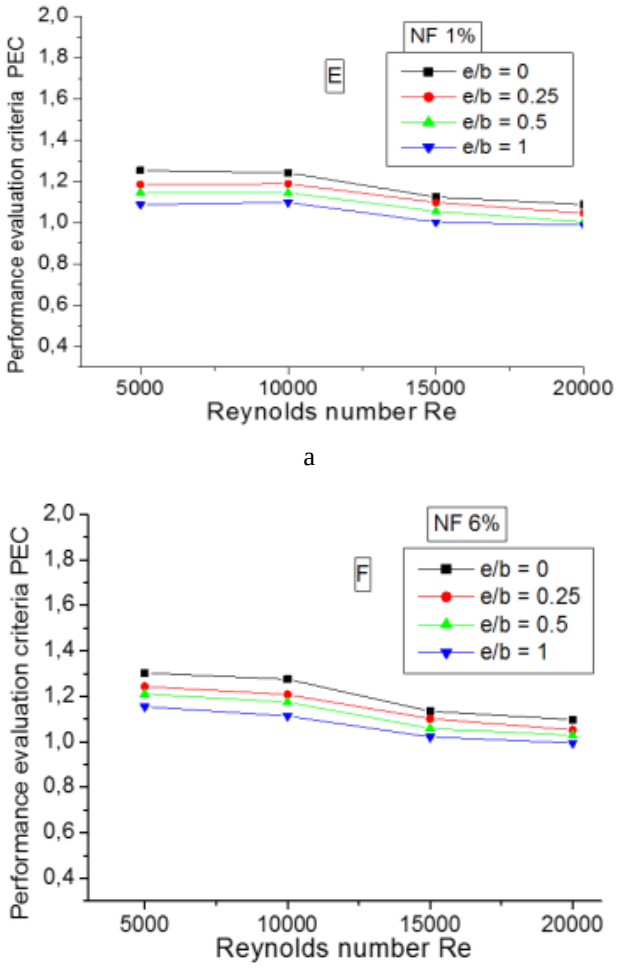

a b

Fig. 7 Effectof space ratio with different Reynolds numbers FEC: (a) NF 1% (b) NF 6%

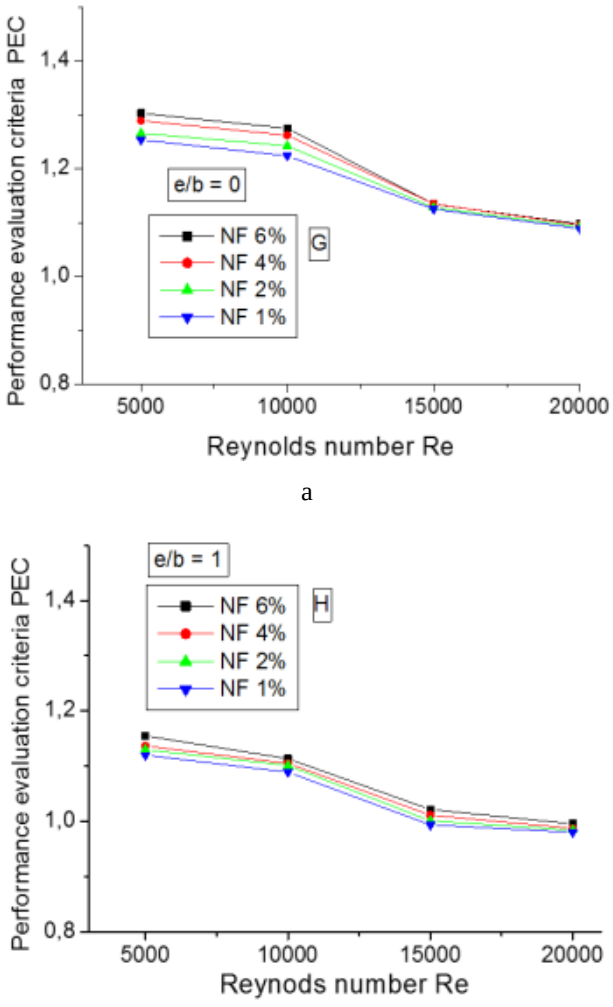

a b

Fig. 8 Effect of volume fraction nanoparticles with different Reynolds numbers FEC: a – *e/b* = 0, b – *e/b* =1

The same indication for the PEC results was noticed in Fig. 7 and Fig. 8. The continuity of undulation rib of the wall gave optimum performance in terms of thermal and hydraulic behavior. it is noted that the increase in the Reynolds number lead to the lowering of the PFC, as well as the profiles of the variation of PFC are almost identical

for the two cases. We noted that the performance evaluation criteria index PEC can written as following [7].

$$PEC = \left(Nu / Nu_0 \right) \Big/ \left(f / f_0 \right)^{1/3}. \quad (8)$$

4.3. Profile of velocity

In Fig. 9, the axial velocity profile is graphed at various x positions, specifically at 0.218, 0.236, 0.254, and 0.272 meters, all within the same test section (L_2). The results indicate a consistent rise in axial velocity as the fluid penetrates deeper into the test channel. This acceleration in fluid flow is evidently attributed to the influence of the wall ribs.

Fig. 10 displays static temperature profiles for various Reynolds numbers, spanning from 5000 to 20000. The thermal enhancement factor is examined by comparing Al_2O_3 nanofluid with water as the working fluid. The utilization of ribbed walls, in contrast to a smooth channel, leads to an increase in Nusselt number and corresponding pressure drop.

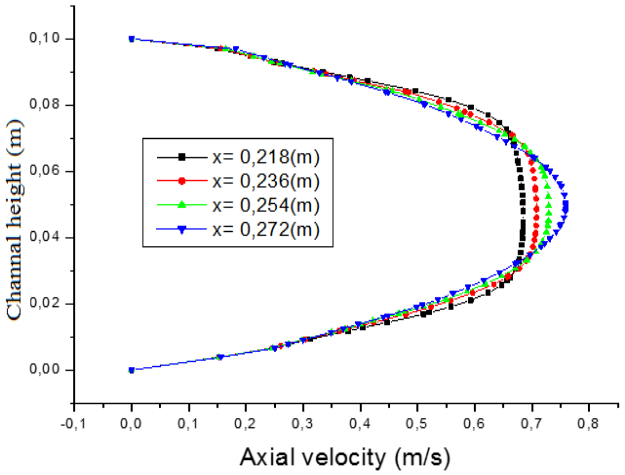

Fig. 9 Axial velocity profile of different position of (x) at Re=5000 for same test section (L_2)

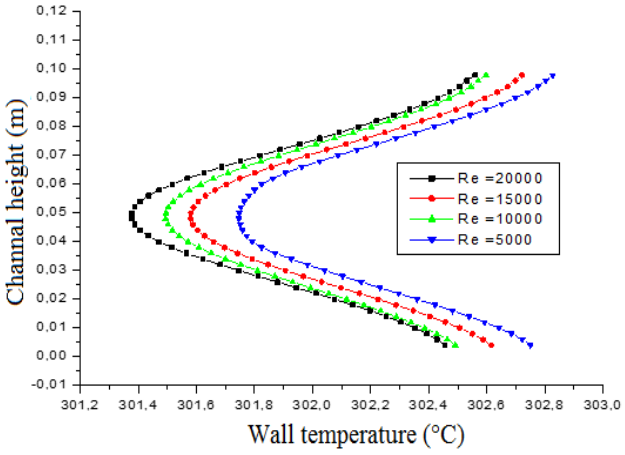

Fig. 10 Profiles of static temperature as function Reynolds number

5. Conclusions

In this study, turbulent flows in forced convection within a channel with a ribbed wall and uniformed heat flow were simulated using the finite volume method with the SIMPLE algorithm. The results indicate that utilizing sinusoidal micro-channels with nanoparticles is a more efficient approach for enhancing heat transfer compared to using nanoparticles with the base fluid in smooth micro-channels. The highest Nusselt number values were observed for nanofluid with a concentration of 1%, with the minimum temperature at the side surfaces of the channel walls and higher values at the channel center, indicating that heat exchange can be intense in areas close to the wall. Furthermore, the friction factor decreases as Reynolds number increases for all channel cases, but increases with higher nanofluid particle concentrations. Lastly, ribbed channels with a rib distance of 0 mm (e/b = 0) produced the highest average Nusselt number for all Reynolds numbers.

References

1. **Ali, A. J.; Tugolukov, E. N.** 2021. Review enhancement of thermal conductivity and heat transfer using carbon nanotube for nanofluids and ionanofluids, Journal of Thermal Engineering 7: 66-90. https://doi.org/10.18186/thermal.843077.
2. **Vanaki Sh. M.; Mohammed H. A**. 2015. Numerical study of nano-fluid forced convection flow in channels using different shaped transverse ribs, International Communications in Heat and Mass Transfer 67: 176-188. https://doi.org/10.1016/j.icheatmasstransfer.2015.07.004.
3. **Ching-chi, W.; Chen C.; Yang Y., Huang K.** 2018. Numerical simulation of turbulent flow forced convection in a twisted elliptical tube, International journal of thermal sciences 132**:** 199-208. https://doi.org/10.1016/j.ijthermalsci.2018.05.028.
4. **Halelfadl, S.; Maré, T; Estellé, P.** (2014). Efficiency of carbon nanotubes water based nanofluids as coolants, Exp Therm Fluid Sci 53: 104-10. https://doi.org/10.1016/j.expthermflusci.2013.11.010.
5. **Ahmadi; A. R.; Zahmatkesh, A., Hatami, M.; Ganji, D. D.** 2014. A comprehensive analysis of the flow and heat transfer for a nanofluid over an unsteady stretching flat plate, Powder Technol 258: 125-33. https://doi.org/10.1016/j.powtec.2014.03.021.
6. **Trisaksri, V; Wongwises, S** 2007. Critical review of heat transfer characteristics of nanofluids. Renew Sustain Energy Rev 11: 512–23. https://doi.org/10.1016/j.rser.2005.01.010.
7. **Goharshadi, E.K.; Ahmadzadeh, H.; Samiee, S.; Hadadian M.** 2013. Nanofluids for Heat Transfer Enhancement – A Review, Physical Chemistry Research 1(1): 1-33. https://doi.org/10.22036/pcr.2013.2791.
8. **Kleinstreuer, C & Feng, Y.** 2011. Experimental and theoretical studies of nanofluid thermal conductivity enhancement: a review. Nanoscale research letters 6(1): 229. https://doi.org/10.1186/1556-276X-6-229.
9. **Lazarus G.** 2015. Nanofluid heat transfer and applications, Journal of Thermal Engineering 1(2): 113-115.

https://doi.org/10.18186/jte.93344.
10. **Lee, S.; Choi, S. U.; Li, S.; Eastman J. A.** 1999. Measuring Thermal Conductivity of Fluids Containing Oxide Nanoparticles, ASME Journal of Heat and Mass Transfer 121(2): 280–289. https://doi.org/10.1115/1.2825978.
11. **Deng, F.; Zheng, Q. S; Wang, L. F.; Nan, C. W.** 2007. Effects of anisotropy, aspect ratio, and nonstraightness of carbon nanotubes on thermal conductivity of carbon nanotube composites, Appl Phys Lett. 90: 21914. https://doi.org/10.1063/1.2430914.
12. **Lazarus, G.; Roy, S., Kunhappan, D.; Cephas, E.; Wongwises, S.** 2015. Heat transfer performance of silver/water nanofluid in a solar flat-plate collector, J Therm Eng. 1: 104-112. https://doi.org/10.18186/jte.29475.
13. **Barbés, B.; Páramo, R; Blanco, E.; Pastoriza-Gallego M. J.; Pineiro M. M.; Legido J. L**. et al. 2013. Thermal conductivity and specific heat capacity measurements of Al 2 O 3 nanofluids, J. Therm Anal Calorim 111: 1615-25. https://doi.org/10.1007/s10973-012-2534-9.
14. **Estellé, P.; Halelfadl S., Maré, T.** 2015. Thermal conductivity of CNT water based nanofluids: Experimental trends and models overview, J. Therm Eng. 1: 381–90. https://doi.org/10.18186/jte.92293.
15. **Rebai, B.** 2023. Contribution to study the effect of (Reuss, LRVE, Tamura) models on the axial and shear stress of sandwich FGM plate (Ti–6A1–4V/ZrO 2) subjected on linear and nonlinear thermal loads, AIMS Materials Science 10(1): 26-39. https://doi.org/10.3934/matersci.2023002.
16. **Tokgöz, N.; Alıç, E.; Kaşka, Ö.; Aksot M. M.** 2018. The numerical study of heat transfer enhancement using AL2O3-water nanofluid in corrugated duct application. https://doi.10.18186/journal-of-thermal-engineering.409655.
17. **Khairul, M. A.; Shah, K.; Doroodchi, E.; Azizian, R.; Moghtaderi, B.** 2016. Effects of surfactant on stability and thermo-physical properties of metal oxide nanofluids, Int J Heat Mass Transf. 98: 778-87. https://doi.org/10.1016/j.ijheatmasstransfr.2016.03.079.
18. **Rebai, B.** et al. 2023. Effect of Idealization Models on Deflection of Functionally Graded Material (FGM) Plate, J. Nano- Electron. Phys. 15(1): 01022-1-01022-5. https://doi.org/10.21272/jnep.15(1).01022.
19. **Hatami, M.; Nouri, R.; Ganji, D. D.** 2013. Forced convection analysis for MHD Al2O3–water nanofluid flow over a horizontal plate, J Mol Liq; 187:294–301. https://doi.org/10.1016/j.molliq.2013.08.008.
20. **Timofeeva, E. V.; Routbort, J. L.; Singh, D.** 2009. Particle shape effects on thermophysical properties of alumina nanofluids, J. Appl Phys 106: 14304. https://doi.org/10.1063/1.3155999.
21. **Bayareh, M.; Nourbakhsh, A.** 2019. Numerical simulation and analysis of heat transfer for different geometries of corrugated tubes in a double pipe heat exchanger, Journal of Thermal Engineering 5: 293-301. https://doi.org/10.18186/thermal.581775.
22. **Rostamani, M.; Hosseinizadeh, S.F.; Gorji, M.; Khodadadi, J.M.** 2010. Numerical study of turbulent forced convection flow of nanofluids in a long horizontal duct considering variable properties, International Communications in Heat and Mass Transfer 37(10): 1426-1431. https://doi.org/10.1016/j.icheatmasstransfer.2010.08.007.
23. **Manca, O.; Nardini, S.; Ricci D.** 2012. A numerical study of nanofluid forced convection in ribbed channels, Applied Thermal Engineering 37: 280-292. https://doi.org/10.1016/j.applthermaleng.2011.11.030.
24. **Gawande, V.B.; Dhoble, A.S.; Zodpe D.B.; Chamoli, S.** 2016. Experimental and CFD investigation of convection heat transfer in solar air heater with reverse L-shaped ribs, Solar Energy 131: 275-295. https://doi.org/10.1016/j.solener.2016.02.040.

B. Litouche, B. Rebai, K. Mansouri

INVESTIGATING THE IMPACT OF FLOW PROFILE ON HEAT TRANSFER IN NANOFLUID FLOW: A NUMERICAL STUDY

S u m m a r y

Assessing the profitability of an energy system requires careful consideration of various factors, including fluid characteristics, geometry shape, and operating conditions. This study investigates the influence of sinusoidal rib shapes, with different space ratios (*e*/*b*) ranging from 0 to 1, on heat transfer in nanofluid flow. The channel's upper surface is subjected to a uniform heat flux, employing Al2O3 nanofluid as the working fluid and varying Reynolds numbers from 5000 to 20000. Additionally, the effect of aluminum nanoparticle volume fraction, ranging from 0 to 6%, is analyzed. Simulation results indicate that the performance of the corrugated surface in the channel is significantly influenced by rib shapes and their geometrical parameters. The highest Performance Evaluation Criteria (PEC) index is achieved for ribs with a space ratio (*e*/*b*) of 0 at Reynolds number of 5000 and a volume fraction of 6% nanoparticles. Furthermore, the average Nusselt number shows an increasing trend with higher particle volume fraction and Reynolds numbers.

Keywords: nanofluid, geometric factor, turbulent flow regime, nanoparticle volume fraction, heat convective transfer.

Received July 15, 2023
Accepted April 15, 2024